J|A|C|S ARTICLES

Published on Web 06/25/2009

Locus-Specific Microemulsion Catalysts for Sulfur Mustard (HD) Chemical Warfare Agent Decontamination

Ian A. Fallis,*,† Peter C. Griffiths,*,† Terence Cosgrove,‡ Cecile A. Dreiss,§ Norman Govan,|| Richard K. Heenan,⊥ Ian Holden,|| Robert L. Jenkins,† Stephen J. Mitchell,|| Stuart Notman,|| Jamie A. Platts,† James Riches,|| and Thomas Tatchell†

School of Chemistry, Cardiff University, Main Building, Park Place, Cardiff, CF10 3AT, U.K., School of Chemistry, University of Bristol, Cantock's Close, Bristol BS8 1TS, U.K., Department of Pharmacy, King's College London, Franklin-Wilkins Building, 150 Stamford Street, London, SE1 9NN, Defence Science Technology Laboratory (DSTL), Porton Down, Salisbury SP4 0JQ, Wilts, U.K., and ISIS Pulsed Neutron & Muon Source, Rutherford Appleton Laboratory, Chilton, Didcot, OX11 0QX, U.K.

Received March 12, 2009; E-mail: fallis@cf.ac.uk

Abstract: The rates of catalytic oxidative decontamination of the chemical warfare agent (CWA) sulfur mustard (HD, bis(2-chlororethyl) sulfide) and a range (chloroethyl) sulfide simulants of variable lipophilicity have been examined using a hydrogen peroxide-based microemulsion system. SANS (small-angle neutron scattering), SAXS (small-angle X-ray scattering), PGSE-NMR (pulsed-gradient spin−echo NMR), fluorescence quenching, and electrospray mass spectroscopy (ESI-MS) were implemented to examine the distribution of HD, its simulants, and their oxidation/hydrolysis products in a model oil-in-water microemulsion. These measurements not only present a means of interpreting decontamination rates but also a rationale for the design of oxidation catalysts for these toxic materials. Here we show that by localizing manganese−Schiff base catalysts at the oil droplet−water interface or within the droplet core, a range of (chloroethyl) sulfides, including HD, spanning some 7 orders of octanol−water partition coefficient (K_{ow}), may be oxidized with equal efficacy using dilute (5 wt. % of aqueous phase) hydrogen peroxide as a noncorrosive, environmentally benign oxidant (e.g., $t_{1/2}$ (HD) $\sim$ 18 s, (2-chloroethyl phenyl sulfide, $C_6H_5SCH_2CH_2Cl$) $\sim$ 15 s, (thiodiglycol, $S(CH_2CH_2OH)_2$) $\sim$ 19 s {20 °C}). Our observations demonstrate that by programming catalyst lipophilicity to colocalize catalyst and substrate, the inherent compartmentalization of the microemulsion can be exploited to achieve enhanced rates of reaction or to exert control over product selectivity. A combination of SANS, ESI-MS and fluorescence quenching measurements indicate that the enhanced catalytic activity is due to the locus of the catalyst and not a result of partial hydrolysis of the substrate.

Introduction

During World War I, the nature of human conflict was changed forever by the large scale deployment of chemical warfare agents (CWAs).[1] As a consequence, the ability to efficiently decontaminate these highly toxic materials,[2] with minimal environmental impact, has since become a global necessity. Of particular concern is the persistence of the potent vesicant bis(2-chloroethyl) sulfide (sulfur mustard, HD, Scheme 1) which renders it a demanding decontamination problem.[3−5] There are several modes of decontamination available for HD including desulfurization,[6] photocatalysis,[7] dehydrohalogenation,[8] aerobic (O_2) oxidations,[9] and by hydrolysis to the low

† Cardiff University.
‡ University of Bristol.
§ King's College London.
|| Defence Science Technology Laboratory.
⊥ Rutherford Appleton Laboratory.

(1) For historical perspectives, see (a) Tucker, J. B. *War of Nerves: Chemical Warfare from World War I to Al-Qaeda*; Pantheon Books: New York, 2006. (b) Coleman, K. *A History of Chemical Warfare Pelgrave*; Macmillan: Basingstoke, 2005. (c) Croddy, E. *Chemical and Biological Warfare*; Springer-Verlag: New York, 2001. (d) Paxman, J.; Harris. R. *A Higher Form of Killing: The Secret History of Chemical and Biological Warfare*; Arrow: London, 2001. (e) McWilliams, J. L.; Steel, R. J. *Gas! The Battle for Ypres, 1915*; Vanwell Publishing Limited: Canada, 1985.

(2) For discussions of sulfur mustard toxicology, see (a) Kales, S. N.; Christiani, D. C. *N. Engl. J. Med.* **2004**, *350*, 800–808. (b) Dacre, J. C.; Goldman, M. *Pharmacol. Rev.* **1996**, *48*, 289–326. (c) Gilman, A.; Philips, F. S. *Science* **1946**, *103*, 409–436.

(3) (a) Marshall, E. *Science* **1984**, *224*, 130–132. (b) Fitch, J. P.; Raber, E.; Imbro, D. R. *Science* **2003**, *302*, 1350–1354. (c) Talmage, S. S.; Watson, A. P.; Hauschild, V.; Munro, N. B.; King, J. *Curr. Org. Chem.* **2007**, *11*, 285–298.

(4) For a key review of early literature, see Yang, Y. C.; Baker, J. A.; Ward, J. R. *Chem. Rev.* **1992**, *92*, 1729–1743.

(5) (a) Smith, B. M. *Chem. Soc. Rev.* **2008**, *37*, 470–478. (b) Eubanks, L. M.; Dickerson, T. J.; Janda, K. D. *Chem. Soc. Rev.* **2007**, *36*, 458–470.

(6) Sorensen, A. C.; Landry, C. C. *Catal. Lett.* **2005**, *100*, 135–138.

(7) Vorontsov, A. V.; Lion, C.; Savinov, E. N.; Smirniotis, P. G. *J. Catal.* **2003**, *220*, 414–423.

(8) Wagner, G. W.; Koper, O. B.; Lucas, E.; Decker, S.; Klabunde, K. J. *J. Phys. Chem. B* **2000**, *104*, 5118–5123.

 10.1021/ja901872y CCC: $40.75

Scheme 1. Structures of (a) Sulfur Mustard (HD), Its Sulfoxide and Sulfone Oxidation Products (HDO, HDO_2) and Thiodiglycol (TDG), (b) Selected HD Simulants, and (c) [MnCl(salen)] Catalysts Used in This Study[a]

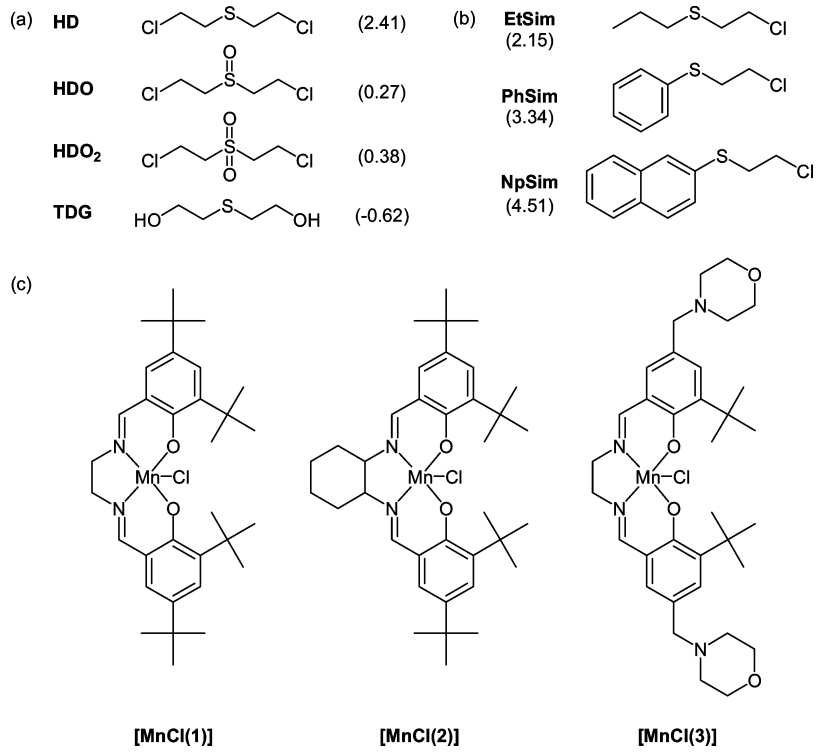

[a] The numbers in parentheses are the calculated[51] log K_{ow} values.

toxicity[10] thiodiglycol (TDG) at metal oxide nanoparticle surfaces and zeolites.[11] However, it is most practical to detoxify bulk HD oxidatively to the sulfoxide (HDO) with liquid decontaminants and herein lays a fundamental chemical challenge: most suitable oxidants are water-soluble, while HD is water immiscible. The water immiscibility, coupled with rheological modification (thickening) employed for some military uses, imbues the agent with environmental persistence[12] and resistance to purely aqueous-based decontamination systems. Such 'phase incompatibility' is often addressed using micellar[13,14] or oil-in-water microemulsion systems to promote the intimate contact of dispersed HD with a water-based oxidant system.[15]

To date the most active liquid decontaminants are arguably the nucleophilic diethylenetriamine/ethylene glycol/monomethyl ether/sodium hydroxide mixtures known as DS2.[4] This system, although an effective broad spectrum decontaminant, is highly corrosive toward many materials, is not suitable for general use, and has been superseded by oxidative systems. The goal in HD oxidative decontamination is typically to achieve conversion to the low toxicity, nonvesicant sulfoxide HDO (Scheme 1), while, if possible, avoiding overoxidation to the vesicant sulfone HDO_2.[16] It is important to note that HDO_2, unlike HDO, is susceptible to hydrolytic decomposition to less toxic materials. Microemulsions and oil swollen micelles are a good choice of decontamination media for HD since the coexistence of aqueous and organic phases means they are not only capable of dispersing thickened HD under conditions of low shear but can also dissolve water-soluble oxidants. One of the most effective HD oxidizing systems is the basic hypochlorite (bleach)-based microemulsions described by Menger and Elington.[17] Although hypochlorite-based systems display very high rates of sulfide oxidation, they also are now deemed both too corrosive and environmentally unacceptable for wide-scale use. It is here that dilute hydrogen peroxide solutions can provide a viable alternative; they are stable, noncorrosive, atom efficient oxidants that are of low environmental impact.[18] However, the uncatalyzed reaction of H_2O_2 and organic sulfides is slow, which necessitates

(9) (a) Livingston, S. R.; Landry, C. C. *J. Am. Chem. Soc.* **2008**, *130*, 13214–13215. (b) Okun, N. M.; Tarr, J. C.; Hilleshiem, D. A.; Zhang, L.; Hardcastle, K. I.; Hill, C. L. *J. Mol. Catal. A* **2006**, *246*, 11–17. (c) Boring, E.; Geletii, Y.; Hill, C. L. *J. Mol. Catal. A* **2001**, *76*, 49–63. (d) Boring, E.; Geletii, Y. V.; Hill, C. L. *J. Am. Chem. Soc.* **2001**, *123*, 1625–1635. (e) Okun, N. M.; Anderson, T. M.; Hill, C. L. *J. Mol. Catal. A* **2003**, *197*, 283–290.

(10) Reddy, G.; Major, M. A.; Leach, G. J. *Int. J. Toxicol.* **2005**, *24*, 435–442.

(11) (a) Wagner, G. W.; Procell, L. R.; O'Connor, R. J.; Munavalli, S.; Carnes, C. L.; Kapoor, P. N.; Klabunde, K. J. *J. Am. Chem. Soc.* **2001**, *123*, 1636–1644. (b) Wagner, G. W.; Bartram, P. W.; Koper, O.; Klabunde, K. J. *J. Phys. Chem. B* **1999**, *103*, 3225–3228. (c) Wagner, G. W.; Bartram, P. W. *Langmuir* **1999**, *15*, 8113–8118. (d) Stout, S. C.; Larsen, S. C.; Grassian, V. H. *Microporous Mesoporous Mater.* **2007**, *100*, 77–86.

(12) (a) Ruhl, C. M.; Park, S. J.; Danisa, O.; Papirmeister, B.; Sidell, F. R.; Edlich, R. F.; Himel, H. N. *J. Emerg. Med.* **1994**, *12*, 159–166. (b) Hao, R. Z.; Cheng, Z. X.; Zhu, H. Y. *J. Phys. Chem. A* **2007**, *111*, 4786–4791. (c) Bartelt-Hunt, S. L.; Barlaz, M. A.; Knappe, D. R. U.; Kjeldsen, P. *Environ. Sci. Technol.* **2006**, *40*, 4219–4225.

(13) Yao, H. R.; Richardson, D. E. *J. Am. Chem. Soc.* **2003**, *125*, 6211–6221.

(14) Jaeger, D. A.; Roberts, T. L.; Zelenin, A. K. *Colloids Surf., A* **2002**, *196*, 209–216.

(15) (a) For a recent review, see Dwars, T.; Paetzold, E.; Oehme, G. *Angew. Chem., Int. Ed.* **2005**, *44*, 7174–7199. (b) Menger, F. M.; Rourk, M. J. *Langmuir* **1999**, *15*, 309–313.

(16) Hirade, J.; Ninomiya, A. *J. Biochem.* **1950**, *37*, 19–34.

(17) (a) Menger, F. M.; Elington, A. R. *J. Am. Chem. Soc.* **1991**, *113*, 9621–9624. (b) Menger, F. M.; Elrington, A. R. *J. Am. Chem. Soc.* **1990**, *112*, 8201–8203.

(18) (a) Wagner, G. W.; Sorrick, D. C.; Procell, L. R.; Brickhouse, M. D.; McVey, I. F.; Schwartz, L. I. *Langmuir* **2007**, *23*, 1178–1186. (b) Sen Gupta, S.; Stadler, M.; Noser, C. A.; Ghosh, A.; Steinhoff, B.; Lenoir, D.; Horwitz, C. P.; Schramm, K. W.; Collins, T. J. *Science* **2002**, *296*, 326–328. (c) Sorokin, A.; Seris, J. L.; Meunier, B. *Science* **1995**, *268*, 1163–1166.

the use of water-soluble peroxide activators[19] or catalysts such as bicarbonate,[20] molybdate,[21] or heteropolytungstates.[22] This illustrates a fundamental dichotomy in HD decontamination, namely that water-soluble oxidants and catalysts can yield effective rates of oxidation of an essentially water immiscible substrate (HD).

Reactivity in micellar or microemulsion systems is often interpreted using the pseudophase model, in which the aqueous continuous phase and micelles or droplets are considered to be a discrete phases[23] while the 'compartmentalization' of reaction media can often have profound effects on rates and product speciation.[24] In this paper we further explore the concept of compartmentalized reaction media further by addressing the following questions: is the *locus* of decontamination within a microemulsion important in determining reaction rate, and thus, can catalysts be engineered to be targeted to specific sites within microemulsions so as to achieve selective decontamination and higher reaction rates?

Experimental Section

HD is listed in Schedule 1 of the Chemical Weapons Convention (CWC) and its production, acquisition, retention or use is strictly controlled. The appropriate CWC National Authority must be informed and any legislative requirements met before working with this chemical. **Caution**: HD and chloroethyl simulants (hemisulfur mustards) are severe vesicants and must be handled with great care in an efficient fume hood.

Solvents were purified by standard literature methods.[25] Deuterated materials were purchased from Cambridge Isotope Laboratories. Full characterization of the microemulsion, synthesis of materials, PGSE NMR and neutron/X-ray scattering measurements, and all other experimental protocols are described in full in the Supporting Information.

Catalysis. Rates of sulfide oxidation in microemulsion solutions of HD and selected simulants were tested at DSTL Porton Down with a gently stirred 20 mL sample volume and monitored in situ for the growth of sulfoxide and sulfone peaks using a Mettler Toledo ReactIR 4000 FT-IR spectrometer with a DiComp (diamond) probe running ReactIR 3.0 software. Details of an analogous experimental procedure have been described elsewhere.[26] Potassium tungstate (Aldrich, 99.99+ %) was used as received. All systems presented here containing hydrogen peroxide, catalysts and simulants were clear, one-phase systems. The oil-soluble catalysts [MnCl(**1**)] and [MnCl(**2**)] were prepared from the parent ligands by adapting the method of Jacobsen et al.[27] [MnCl(**3**)] was synthesized by the condensation of ethylenediamine and the appropriate salicylaldehyde, which was prepared by adapting the procedure of Miller et al.[28] The simulants 2-chloroethyl ethyl sulfide (here denoted EtSim, also known as "CEES"), 2-chloroethyl phenyl sulfide (here denoted PhSim, also known as "CEPS"), and thiodiglycol (TDG) were purchased from Aldrich and used as received. 2-Chloroethyl 2-naphthyl sulfide (here denoted NpSim) was prepared under basic conditions from 2-mercaptonaphthalene and a large excess dichloroethane. Sulfoxides and sulfones for diffusion coefficient measurements were prepared by oxidation of the sulfide using 1 (sulfoxide) or 2 equivalents (sulfone) of sodium perborate by the method of McKillop and Tarbin.[29]

Results and Discussion

HD and Simulant Oxidation: Water- and Oil-Soluble Catalysts. In order to probe the site of sulfide oxidation within a microemeulsion, a number of catalysts and sulfides of varying lipophilicity were prepared. In such an approach, it is possible to match or mismatch the sites to which the catalysts and substrates predominantly distribute themselves and hence determine the importance of partitioning phenomena in reactivity. The rates (expressed as half-lives, $t_{1/2}$) of sulfide oxidation of HD and a range of simulants in the toluene−butanol−sodium dodecylsulfate (SDS)−water microemulsion (here denoted SDS5T) by dilute hydrogen peroxide, were quantified by in situ FT-IR measurements via the growth of sulfoxide and sulfone peaks (Table 1). The microemulsion formulation was chosen, as it has a track record of being able to disperse HD under conditions of low shear. Furthermore, Bunton et al. have suggested that in sulfide oxidations, the reaction transition state are likely to bear a fractional positive charge on sulfur,[30] and hence an anionic microemulsion is a logical choice for catalytic oxidations. Group VI oxo-anions are known to be efficient hydrogen peroxide activators in sulfide oxidation,[21] while oil-soluble alkene epoxidation catalysts[31] such as [MnCl(**2**)] have not been used to date in this role have been shown to be effective in the asymmetric H_2O_2 oxidation of sulfides to sulfoxides.[32,33] Hence, tungstate (as K_2WO_4) and the hydrophobic Mn(III) salen complexes [MnCl(**1**)] and [MnCl(**2**)] (Scheme 1c) were used as water and oil soluble hydrogen peroxide activation catalysts, respectively. Tungstate was chosen over the more widely applied molybdate[21] to facilitate heavy atom fluorecscence quenching (vide infra). It should be noted that in water/cosolvent mixtures (e.g., $MeO(CH_2)_2OH$) the catalysts employed, where sufficiently soluble, were of low activity.

(19) Wagner, G. W.; Yang, Y.-C. *Ind. Eng. Chem. Res.* **2002**, *41*, 1925–1928.

(20) (a) Balagam, B.; Richardson, D. E. *Inorg. Chem.* **2008**, *47*, 1173–1178. (b) Regino, C. A. S.; Richardson, D. E. *Inorg. Chim. Acta* **2007**, *360*, 3971–3977. (c) Richardson, D. E.; Regino, C. A. S.; Yao, H. R.; Johnson, J. V. *Free Radical Biol. Med.* **2003**, *35*, 1538–1550. (d) Richardson, D. E.; Yao, H. R.; Frank, K. M.; Bennett, D. A. *J. Am. Chem. Soc.* **2000**, *122*, 1729–1739.

(21) (a) Yunes, S. J.; Gillitt, N. D.; Bunton, C. A. *Colloid Surf., A* **2006**, *281*, 1–7. (b) Chiarini, M.; Bunton, C. A. *Colloids Surf., A* **2004**, *245*, 177–182. (c) Chiarini, M.; Cerichelli, G.; Foroudian, H. J.; Gillitt, N. D.; Yunes, S. F.; Bunton, C. A. *Langmuir* **2004**, *20*, 5201–5208. (d) Chiarini, M.; Bunton, C. A. *Langmuir* **2002**, *18*, 8806–8812. (e) Chiarini, M.; Gillitt, N. D.; Bunton, C. A. *Langmuir* **2002**, *28*, 3836–3842. (f) Bunton, C. A.; Gillitt, N. D. *J. Phys. Org. Chem.* **2002**, *15*, 29–35. (g) Wagner, G. W.; Procell, L. R.; Yang, Y. C.; Bunton, C. A. *Langmuir* **2001**, *17*, 4809–4811.

(22) (a) Kozhevnikov, I. V. *Chem. Rev.* **1998**, *98*, 171–198. (b) Neumann, R. *Prog. Inorg. Chem.* **1998**, *47*, 317–370. (c) Phan, T. D.; Kinch, M. A.; Barker, J. E.; Ren, T. *Tetrahedron Lett.* **2005**, *46*, 397–400. (d) Kholdeeva, O. A.; Maksimov, G. M.; Maksimovskaya, R. I.; Kovaleva, L. A.; Fedotov, M. A.; Grigoriev, V. A.; Hill, C. L. *Inorg. Chem.* **2000**, *39*, 3828–3837.

(23) For a review of the pseudophase model see, Bunton, C. A. *Adv. Colloid Interface Sci.* **2006**, *123−126*, 333–343.

(24) For an elegant example, see Chen, J.; Körner, S.; Craig, S. L.; Rudkevich, D. M.; Rebek, J., Jr. *Nature* **2002**, *415*, 385–386.

(25) Perrin, D. D. Amarego, W. F. A. *Purification of Laboratory Chemicals*; Pergamon: Oxford, 1988.

(26) Hay, R. W.; Clifford, T.; Govan, N. *Transition Met. Chem.* **1998**, *23*, 619–624.

(27) Larrow, J. F.; Jacobsen, E. N.; Gao, Y.; Hong, Y.; Nie, X.; Zepp, C. M. *J. Org. Chem.* **1994**, *59*, 1939–1942.

(28) Miller, H. A.; Laing, N.; Parsons, S.; Parkin, A.; Tasker, P. A.; White, D. J. *J. Chem. Soc., Dalton Trans.* **2000**, 3773.

(29) McKillop, A.; Tarbin, J. A. *Tetrahedron Lett.* **1983**, *24*, 1505–1508.

(30) Blaskó; Bunton, C. A.; Foroudian, H. J. J. *Colloid Interface Sci.* **1995**, *175*, 122–130.

(31) Zhang, W.; Loebach, J. L.; Wilson, S. R.; Jacobsen, E. N. *J. Am. Chem. Soc.* **1990**, *112*, 2801–2803.

(32) Ueno, T.; Koshiyama, T.; Ohashi, M.; Kondo, K.; Kono, M.; Suzuki, A.; Yamane, T.; Watanabe, Y. *J. Am. Chem. Soc.* **2005**, *127*, 6556–6562.

(33) (a) Palucki, M.; Hanson, P.; Jacobsen, E. N. *Tetrahedron Lett.* **1992**, *33*, 7111–7114. (b) Noda, K.; Hosoya, N.; Yanai, K.; Irie, R.; Katsuki, T. *Tetrahedron Lett.* **1994**, *35*, 1887–1890. (c) Nakajima, K.; Kojima, M.; Fujita, J. *Chem. Lett.* **1986**, 1483–1486.

Table 1. Half-Lives ($t_{1/2}$, seconds, ±10%) for the Formation of Sulfoxide and/or Sulfone in the Catalyzed H_2O_2 Oxidation of Mustard (HD) or Simulant, in the Presence of Toluene/Butanol/SDS Microemulsion Droplets[a]

	agent or simulant	$[H_2O_2]$ (wt. % of H_2O phase)	catalyst (s)	[catalyst] mM	$t_{1/2}$ (s) (sulfoxide)	$t_{1/2}$ (s) (sulfone)
1	HD	1	K_2WO_4	2.0	260	not observed
2		1	[MnCl(**1**)]	2.0	not observed	not observed
3		5	K_2WO_4	2.0	200	not observed
4		5	K_2WO_4	4.0	100	600
5		5	[MnCl(**1**)]	2.0	120	not observed
6		15	[MnCl(**1**)]	0.8	40	200
7		5	[MnCl(**2**)]	2.0	390	not observed
8		30	[MnCl(**2**)]	0.2	400	not observed
9		15	[MnCl(**2**)]	0.8	210	not observed
10		5	[MnCl(**3**)]	2.0	18	43
11		5	[MnCl(**1**)] + [MnCl(**3**)]	2.0[b]	30	60
12	EtSim	5	K_2WO_4	2.0	100	680
13		5	[MnCl(**1**)]	2.0	100	not observed
14	PhSim	5	K_2WO_4	2.0	~1200	not observed
15		5	[MnCl(**1**)]	2.0	90	280
16		5	[MnCl(**3**)]	2.0	15	45
17		5	[MnCl(**1**)] + [MnCl(**3**)]	2.0[b]	20	85
18	NpSim	5	K_2WO_4	2.0	not observed	not observed
19		5	[MnCl(**1**)]	2.0	100	200
20		30	[MnCl(**2**)]	0.2	1000	not observed
21	TDG	5	K_2WO_4	2.0	11[c]	630
22		5	[MnCl(**1**)]	2.0	110	not observed
23		5	[MnCl(**2**)]	2.0	170	not observed
24		5	[MnCl(**3**)]	2.0	38	36

[a] Reactions were performed at 21°C on 200 μL of HD or simulant, with the exception that 357 mg of NpSim was used. The total sample volume was 20 mL in gently stirred reaction vessels. The pH range for all reactions was 8.9−9.2. 1 wt. % H_2O_2 (aq phase) ≈ 0.22 M total $[H_2O_2]$. [b] Mixed catalyst runs; total catalyst concentration = 2.0 mM. [c] Too rapid to fit exponential to IR data, $t_{1/2}$ estimated from time taken to reach half-maximum absorbance.

From the relative rates of oxidation of HD-catalyzed by K_2WO_4 (entry 1) and [MnCl(**1**)] (entry 2), it can be seen that at very low peroxide concentrations tungstate remains active as a catalyst while [MnCl(**1**)] displays little or no activity. At higher peroxide concentrations (5%), the tungstate anion (entries 3 and 4) displayed good activity, while at higher loadings [MnCl(**1**)] became an effective catalyst (entry 5). These results show that [MnCl(**1**)] is capable of catalyzing HD oxidation in the oil phase, implying that oxo transfer from peroxide to lipophilic catalysts can occur across the oil−water interface. This is fundamentally different from phase transfer catalysis since H_2O_2 is not transported into the microemulsion droplet core by the catalysts. Indeed, Richardson *et al.* have shown that the partition coefficient of H_2O_2 into the Stern layer, albeit for a cationic micellar system, has an upper limit of ~2.[13] These rates of oxidation are sufficiently high to be of potential future use and, given the low concentration of H_2O_2, low catalyst loading, and the fact that the microemulsion primary component is water, compare well to previously reported molybdate-catalyzed systems with 50% H_2O_2 as the aqueous component.[21g] At increased catalyst loadings of tungstate (entry 4) and higher peroxide concentrations with [MnCl(**1**)] (entry 6) overoxidation to sulfone (HDO_2) was observed. This result is important, as it demonstrates that [MnCl(**1**)] is capable of catalyzing sulfone formation. This suggests that the selectivity observed at lower oxidant loadings arises from the use of a compartmentalized reaction medium, since no phase separation was observed.

In experiments using half-mustard simulants (entries 12−20) the activity noted for K_2WO_4 and [MnCl(**1**)] with HD is comparable to that observed for the widely adopted simulant 2-chloroethyl ethyl sulfide (EtSim, entries 12, 13). However, in examining more lipophilic simulants a new reactivity pattern was seen to emerge; in the oxidation of 2-chloroethyl phenyl sulfide (PhSim) using K_2WO_4 (entry 14) and [MnCl(**1**)] (entry 15) the former affords a low reaction rate, while in the case of the oil soluble [MnCl(**1**)] rapid oxidation was observed, not only to the desired sulfoxide product (PhSimO) but also further conversion to the sulfone ($PhSimO_2$). The importance of the relative *locus* of catalyst and substrate within the microemulsion is underpinned by the lack of activity of water-soluble tungstate on the oxidation of the very lipophilic NpSim (entry 18). Comparing the oxidation of HD, EtSim, PhSim, and NpSim under common reaction conditions, it is noted that in all cases [MnCl(**1**)] is an effective catalyst (entries 5, 13, 15, and 19, respectively) with consistent activity ($t_{1/2}$ {sulfoxide} ~ 100s), irrespective of simulant structure. In contrast, K_2WO_4 only displayed significant activity against HD and EtSim (entries 3, 12, 14, and 18), with the rates decreasing with increasing simulant lipophilicity. Further, the more oil-soluble simulants undergo overoxidation to the sulfone when oil-soluble catalysts were used (entries 15, 19) while the less lipophilic HD and EtSim were overoxidized by the water-soluble tungstate catalyst (entries 4, 17). In those reactions using the more hindered [MnCl(**2**)] (Jacobsen's catalyst,[32] entries 7−9), the same general trends as for [MnCl(**1**)] are observed, except that the reactions tended to be considerably slower and were unaffected by increases in peroxide concentration. Most significantly, these reactions were completely selective in favor of sulfoxide (HDO) formation (entry 9). These observations are commensurate with the increased steric bulk of [MnCl(**2**)]. For the water-soluble HD hydrolysis product thiodiglycol (TDG, Scheme 1), as expected, very high activity was observed in the case of K_2WO_4 (entry 21). Surprisingly high activity is also observed in the cases of the droplet-confined [MnCl(**1**)] (entry 22) and [MnCl(**2**)] which suggests that TDG has some propensity to penetrate the interfacial region. Both TDG and thiodiglycol sulfoxide (TDGO) have comparable measured partitioning behavior, and thus the observed selectivity in favor of sulfoxide

formation reflects the generally observed slower oxidation of a sulfoxide to a sulfone.

As a footnote to this part of the catalysis studies, it was speculated that, given the activity of K_2WO_4 and [MnCl(**1**)] as water- and oil-soluble catalysts respectively, that *both* catalysts may be used to achieve additive rates of catalysis. However, when this experiment was attempted, an overall *lower* rate ($t_{1/2}$(HD) > 1200 s) of sulfide oxidation was achieved. We can speculate that the tungstate or peroxotungstate anion may coordinate via an oxo or peroxo bridge to the Mn center and mutually inhibit both aqueous- and oil-phase catalysis.

SANS and PGSE-NMR Studies. Loci of Agents and Oxidation Products. In order to rationalize the above rate data, it is necessary to understand the partitioning of substrates, product, and catalysts within the microemulsion. Hence, parallel small-angle neutron scattering (SANS) and pulsed-gradient spin-echo NMR (PGSE-NMR) studies were undertaken to establish simulant and catalyst distribution within the microemulsion. While these techniques are ideally suited to examining partitioning phenomena in microemulsions, they suffer from relatively long acquisition times and therefore cannot be used to directly examine the above catalysis. In addition, this issue could not be simply resolved by lowering catalyst or oxidant concentration to yield slower reaction turnover, since the onset of agent hydrolysis with longer reaction times would change the composition of the system and alter the partitioning of substrates. The hydrolysis of HD in aqueous media occurs in tens of minutes to hours,[4,34,35] a time scale which is comparable to the PGSE-NMR and SANS experiment duration (≈30 min), but it is too slow by at least 1 order of magnitude to play a significant role in the catalysis described above. However, hydrolysis does provide a model of a system that *evolves* within the SANS and PGSE-NMR experimental time scales where nonpolar sulfides are converted to polar species via alkyl chloride to alcohol hydrolysis and sulfonium ion formation. This presents a useful model for the more rapidly catalyzed sulfide to sulfoxide oxidation reactions.

SANS.[36] A complete and detailed characterization of the base microemulsion is essential to interpret both the catalysis results and the NMR studies (see below). This has been achieved with a contrast variation small-angle scattering study[37] involving both neutrons and X-rays. Contrasts pertaining to core-only, shell-only, and core + shell neutron scattering, in combination with X-ray scattering have been recorded. A model has been invoked to fit all contrasts simultaneously comprising an oil core (toluene) surrounded by a shell of surfactant (SDS) and cosurfactant (*n*-butanol) (Supporting Information). Further, it was necessary to study various dilutions of the parent microemulsion as the presence of the intense structure peak rendered the simultaneous analysis very sensitive to subtle differences in the composition of the system (volume changes due to protic/deuterium substitution, addition of even low levels of catalyst or simulant). Notwithstanding these experimental difficulties, the model fully described the scattering patterns, Figure 1, indicating no significant change in droplet size of the base microemulsion ($R_{droplet} \sim 24$ Å) on diluting with D_2O either for ×3 dilution ($R_{droplet} \sim 22$ Å) or ×5 dilution ($R_{droplet} \sim 24$ Å). These estimates are in good agreement with the values obtained from the PGSE-NMR analysis, once the effects of the viscosity on the droplet diffusion have been corrected for.

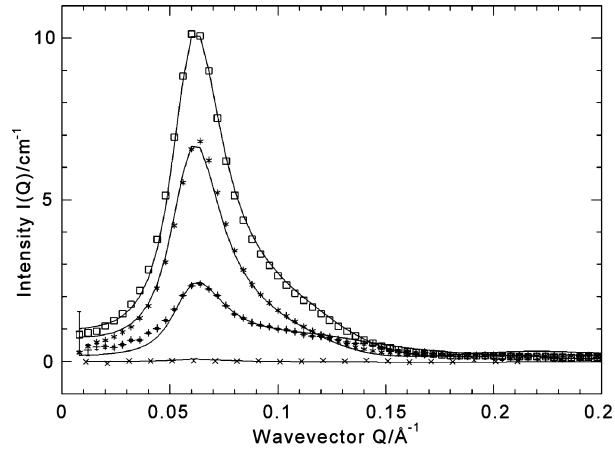

Figure 1. SANS contrast variation study from a 3-fold dilution of SDS5T. Contrasts refer to drop (∅), shell (*), core (+, scaled ×5), and perdeuterated microemulsion (×, scaled ×5), showing the simultaneous fit to the parameters presented in Table S1. The data have been binned in twos for clarity.

Taken together, these results clearly demonstrate that the microemulsion droplets are indeed small and not that much bigger than an SDS micelle ($R_{micelle} \sim 20$ Å). The system may be better described as toluene-swollen SDS micelles. Thus, the generally good rates of catalysis observed in the current microemulsion may be explained via the large oil−water contact area. The thickness of the shell is approximately 10 Å, approximately half the length of a fully extended dodecyl chain including the sulfate headgroup. Further, and arguably more importantly, the assumed distribution of the various components—toluene as the core, SDS and butanol as the shell—are consistent with the actual distribution. The absolute value of the scattering observed is, however, slightly less than the model predicts, logically reflecting the fact that some monomeric SDS and butanol will reside in the water phase. Similar analyses of the microemulsion in the presence of the simulants and catalysts showed that the undiluted microemulsion and the one at lower dilution (×3) were unaffected by the presence of 1 wt % "additive", in good agreement with the only small variation in diffusion coefficient (see below) on inclusion of the additive. Not surprisingly, the stability of the more highly diluted microemulsion (×5) was rather more sensitive to the presence of the additive. A full description of the analysis is presented in the Supporting Information.

The SANS of 1 wt. % dispersions of EtSim, PhSim, and [MnCl(**1**)] in a perdeuterated (full contrast match) sample of microemulsion are shown as a semilog representation in Figure 2, to emphasize the changes in scattering intensity. Here the lipophilic simulant PhSim and catalyst [MnCl(**1**)] were found to partition into the oil phase and thus manifest a peak in the

(34) Logan, T. P.; Sartori, D. A. *Toxicol. Mech. Methods* **2003**, *13*, 235–240.
(35) (a) Yang, Y.-C.; Szafraniec, L. L.; Beaudry, W. T.; Wagner, J. R. *J. Org. Chem.,* **1988**, *53*, 3293–3297. (b) McManus, S. P.; Neamati-Mazraeh, N.; P Hovanes, P. A.; Paley, M. S.; Harris, J. M. *J. Am. Chem. Soc.* **1985**, *107*, 3393–3395. (c) Wilson, R. E.; Fuller, E. W.; Schur, M. O. *J. Am. Chem. Soc.* **1922**, *44*, 2762–2783. (d) Wilson, R. E.; Fuller, E. W.; Schur, M. O. *J. Am. Chem. Soc.* **1922**, *44*, 2867–2878.
(36) For examples of the application of SANS in micelle and microemulsion analyses, see (a) Silas, J. A.; Kaler, E. W. *J. Colloid Interface Sci.* **2003**, *257*, 291–298. (b) Hellweg, T. *Curr. Opin. Colloid Interface Sci.* **2002**, *7*, 50–56. (c) Castelletto, V.; Hamley, I. W. *Curr. Opin. Colloid Interface Sci.* **2002**, *7*, 167–172. (d) Strey, R.; Glatter, O.; Schubert, K. V.; Kaler, E. W. *J. Chem. Phys.* **1996**, *105*, 1175–1188.
(37) For a recent example, see Wang, L. J.; Mutch, K. J.; Eastoe, J.; Heenan, R. K.; Dong, J. F. *Langmuir* **2008**, *24*, 6092–6099.

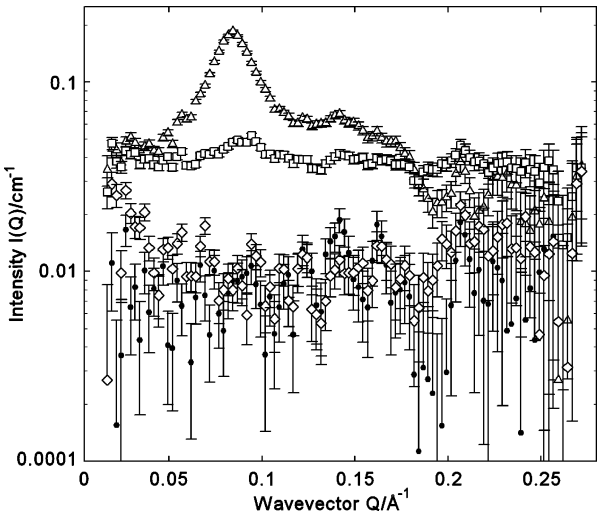

Figure 2. Small-angle neutron scattering from an undiluted perdeuterated SDS 5T microemulsion control (●); containing 1 wt. % EtSim (◇), 1 wt. % PhSim (□), and catalyst (1 wt. % [MnCl(**1**)], △); a peak is indicative of localization (solubilization) into the microemulsion droplet.

SANS pattern, Figure 2, reflecting the underlying structure of the microemulsion and its structure peak (cf. Figure 1). The intensity and position of a structure peak, as observed in Figures 1 and 2, are complex functions of the droplet composition, charge, and interdroplet separation (i.e., concentration). The relatively better defined structure peak observed for [MnCl(**1**)] may be contrasted with a cursory interpretation of Figure 2, and correcting for the relative concentrations and scattering length densities would suggest that the structure peak observed in the PhSim case is perhaps weaker than expected. A contributing factor will certainly be the onset of hydrolysis to $PhSCH_2CH_2OH$ which, although oil soluble, will lead to a perturbation of droplet composition. In addition, it is not unreasonable given the propensity of chloroethyl sulfides to self-react[4,8,38] that generation of sulfonium species such as $PhS^+(CH_2CH_2SPh)CH_2CH_2OH$ occurs and that these ionic materials will partition into the water phase. This analysis is supported by the complete absence of a structure peak in the EtSim data (Figure 2), which is indicative effectively of no partitioning of the agent into the microemulsion droplet. Subsequent electrospray ionization mass spectrometry analysis[35a,39] (ESI-MS, Supporting Information) of EtSim microemulsion dispersed samples prepared in an identical manner show that EtSim undergoes hydrolyses to the expected alcohol (i.e., $HO(CH_2)_2SEt$), but also forms the cationic sulfonium salts $X(CH_2)_2S^+(Et)CH_2CH_2SEt$ (X = OH, Cl) and somewhat unexpectedly the 1-butanol addition product $EtSCH_2CH_2S^+(Et)CH_2CH_2OBu^n$. $EtSCH_2CH_2S^+(Et)CH_2CH_2OC_4D_9$ is formed in the case of deuterated microemulsions. These species are much more hydrophilic than EtSim and hence, at this level of loading, would partition into both the Stern layer and aqueous regions, explaining the absence of large scale structures in the SANS data. It is interesting to note that Menger and Erlington proposed that in hypochlorite-based microemulsions containing 1-butanol, an alkyl hypochlorite was the active oxidant.[17] In the current example we suggest that the cosurfactant also adopts a noninnocent role, acting with enhanced nucleophilicity toward interfacially bound episulfonium species to afford 1-butanol-derived alcoholysis products. Restrictions on the use of HD prevented a SANS study on HD itself, but a mass spectroscopic analysis of HD in the microemulsion indicated comparable but more complex behavior with the identification of at least six sulfonium hydrolysis and five butanolysis products (see ref 35a and Supporting Information). Further, in a departure from the behavior of EtSim, even after several hours in microemulsion solution, sulfonium species bearing chloroalkyl functionalities still persisted.

It can be deduced that polarity changes arising from hydrolysis (or alcoholysis) have significant effects on mustard-derived species distribution within a microemulsion system. To examine this effect in the context of the catalysis results, the speciation and distribution of HD, simulants, and oxidation products within microemulsions must be established. PGSE-NMR was used to provide an independent measure of the partitioning of the substrates, products, and catalysts within the microemulsion via population-weighted self-diffusion coefficients (D_s).[40]

PGSE-NMR. The PGSE-NMR experiment is commonly used to extract emulsion droplet sizes and the distribution of species within a microemulsion.[41] In the PGSE-NMR experiment, the attenuation of the NMR signal gives information on molecular displacement along the gradient direction (z axis) that has occurred during the time period Δ. This can be related to the self-diffusion coefficient D_s. To date PGSE-NMR methods have been used to examine aggregation in micellar or polymeric systems,[42] complex mixtures,[43] liquid-crystals,[44] fluid transport in porous material,[45] aggregation of zwitterionic materials,[46] ion-pairing in inorganic systems,[47] host−guest complexes,[48] but only a relatively small number of catalytic systems.[49,50] It is possible

(38) Stahmann, M. A.; Fruton, J. S.; Bergmann, M. *J. Org. Chem.* **1946**, *11*, 704–718.
(39) (a) For a related study, see Rohrbaugh, D. K.; Yang, Y. C. *J. Mass Spectrom.* **1997**, *32*, 1247–1252.
(40) Söderman, O.; Stilbs, P. *Prog. Nucl. Magn. Reson. Spectrosc.* **1994**, *25*, 445–482.
(41) Sjoblom, J., Ed. *Emulsions and Emulsion Stability*; Surfactant Science Series,Marcel Dekker: New York, 1996.
(42) (a) Alami, E.; Abrahmsen-Alami, S.; Eastoe, J.; Heenan, R. K. *Langmuir* **2003**, *19*, 18–23. (b) Fanun, M.; Wachtel, E.; Antalek, B.; Aserin, A.; Garti, N. *Colloids Surfaces A* **2001**, *180*, 173–186.
(43) (a) Nilsson, M.; Morris, G. A. *Chem. Commun.* **2007**, 933–935. (b) Stchedroff, M. J.; Kenwright, A. M.; Morris, G. A.; Nilsson, M.; Harris, R. K. *Phys. Chem. Chem. Phys.* **2004**, *6*, 3221–3227.
(44) Dvinskikh, S. V.; Furo, I. *J. Chem. Phys.* **2001**, *115*, 1946–1950.
(45) Callaghan, P. T.; Coy, A.; Macgowan, D.; Packer, K. J.; Zelaya, F. O. *Nature* **1991**, *351*, 467–469.
(46) Kang, H.; Facchetti, A.; Jiang, H.; Cariati, E.; Righetto, S.; Ugo, R.; Zuccaccia, C.; Macchioni, A.; Stern, C. L.; Liu, Z. F.; Ho, S. T.; Brown, E. C.; Ratner, M. A.; Marks, T. J. *J. Am. Chem. Soc.* **2007**, *129*, 3267–3286.
(47) For reviews, see. (a) Pregosin, P. S. *Prog. Nucl. Magn. Reson. Spectrosc.* **2006**, *49*, 261–288. (b) Pregosin, P. S.; Kumar, P. G. A.; Fernandez, I. *Chem. Rev.* **2005**, *105*, 2977–2998. (c) Kumar, P. G. A.; Pregosin, P. S.; Goicoechea, J. M.; Whittlesey, M. K. *Organometallics* **2003**, *22*, 2956–2960. (d) Burini, A.; Fackler, J. P.; Galassi, R.; Macchioni, A.; Omary, M. A.; Rawashdeh-Omary, M. A.; Pietroni, B. R.; Sabatini, S.; Zuccaccia, C. *J. Am. Chem. Soc.* **2002**, *124*, 4570–4571.
(48) (a) Cohen, Y.; Avram, L.; Frish, L. *Angew. Chem., Int. Ed.* **2005**, *44*, 520. (b) Atkinson, C. E.; Aliev, A. E.; Motherwell, W. B. *Chem.—Eur. J.* **2004**, *9*, 1714. (c) Avram, L.; Cohen, Y. *J. Org. Chem.,* **2002**, *67*, 2639.
(49) (a) van de Coevering, R.; Alfers, A. P.; Meeldijk, J. D.; Martinez-Viviente, E.; Pregosin, P. S.; Gebbink, R. J. M. K.; van Koten, G. *J. Am. Chem. Soc* **2006**, *128*, 12700–12713. (b) Zuccaccia, C.; Stahl, N. G.; Macchioni, A.; Chen, M. C.; Roberts, J. A.; Marks, T. J. *J. Am. Chem. Soc.* **2004**, *126*, 1448. (c) Drago, D.; Pregosin, P. S.; Pfaltz, A. *Chem. Commun.* **2002**, 286.
(50) Ludwig, M.; Kadyrov, R.; Fielder, H.; Haage, K.; Selke, R. *Chem. Eur. J.* **2001**, *7*, 3298.

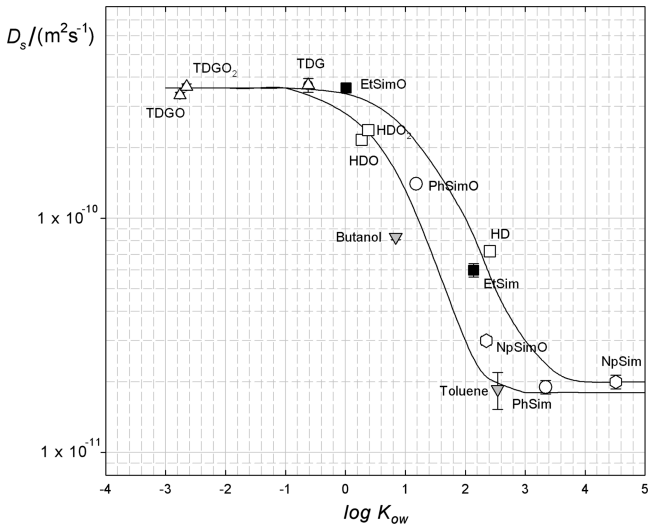

Figure 3. Partitioning of agents employed in the catalysis studies and selected microemulsion components within SDS5T as a function of the measured self-diffusion coefficients (D_s) and calculated[51] octanol−water partition coefficients (K_{ow}). The solid lines indicate any expected variation in measured diffusion coefficient due to the perturbing effects of the additional oil phase on the swollen micelle droplets ($R \sim 2.2$ nm).

to extract the value of the "local" (i.e., inside the droplet) self-diffusion coefficient of the dispersed phase, but the focus here is to quantify the partitioning of species of interest. In the current system the advantage of using microemulsions, as opposed to micellar systems, is that even though the catalyst molecules may be relatively large and lipophilic, the phase stability is not likely to be perturbed by the low concentrations of the catalyst dissolved in the larger core droplet of the oil phase. Further, diffusion coefficients not only yield size information in microemulsions but also directly reflect the partitioning of a particular species within the system. A species with mobility comparable to that of the droplet will be largely associated with the dispersed phase, while hydrophilic materials will exhibit similar mobilities to those observed in simple aqueous solutions. Therefore, in microemulsion media, intermediate D_s values reflect an environment-weighted average and thus may be equated to real, as opposed to calculated, partition coefficients. In order to correlate catalyst activity and agent *loci*, the partitioning was determined within microemulsion media via measurements of agent and simulant self-diffusion (D_s) coefficients. Toluene and mesitylene were used as probes to quantify the diffusion coefficient of the microemulsion droplet.

The D_s values of a broad range of organic sulfides, including HD, HD simulants, and their oxidation products, were measured in a perdeuterated analogue of the microemulsion used in the catalysis experiments described above. In order to identify chemically significant deviations from octanol−water partitioning behavior, these experimentally determined values of mobility were plotted as function of calculated[51] octanol−water partition coefficients (K_{OW}) values (Figure 3). It is apparent from these data that water-miscible materials such as thiodiglycol (TDG, $S(CH_2CH_2OH)_2$) have D_s values approaching those observed in aqueous solution and hence are located predominantly in the water phase while, as expected, droplet constrained species such as PhSim and NpSim diffuse more slowly and have the similar low D_s values to those of toluene in the emulsion core. In contrast, and despite their apparent highly lipophilic nature, HD ($D_s = 3.2 \times 10^{-11}$ m^2 s^{-1}) and EtSim ($D_s = 6.0 \times 10^{-11}$ m^2 s^{-1}) diffuse significantly more rapidly than the oil soluble PhSim and NpSim, having intermediate D_s values more typical of cosurfactants (D_s (BuOH) $= 8.3 \times 10^{-11}$ m^2 s^{-1}). Although the higher mobility implies a lower real K_{ow} value, the droplet core and interface diffuse as a whole, and hence this data cannot distinguish an interfacially bound species from one dissolved within the core of the microemulsion. However, D_s values reflect the weighted average of all environments (droplet, interface, and aqueous phases) the agent is exposed to, and we deduce from its relatively high effective D_s value that HD has a higher interfacial exposure, in comparison to more lipophilic materials. Hence, good rates of decontamination of HD with *both* water- and oil-soluble catalysts should be possible and are indeed observed. This is confirmed by considering the high activity of K_2WO_4 for HD and EtSim oxidation, despite being localized wholly in the aqueous phase, and its poor activity against the more lipophilic PhSim and NpSim.

The significance of the relative locations of catalyst and substrate is evidenced by considering the very high mobilities of sulfoxides relative to those of their parent sulfides. The oxidation of HD to HDO converts a nonpolar sulfide to a dipolar, water-soluble sulfoxide, resulting in a significant increase in mobility (D_s {HDO} $= 7.2 \times 10^{-10}$ m^2 s^{-1}), and hence HDO encounters greater exposure to the aqueous phase. At catalyst loadings where the rates of sulfoxide oxidation for water and oil soluble catalysts are comparable (e.g., Table 1, entries 4 and 5), the increased exposure of HDO to the aqueous phase results in overoxidation to the sulfone (HDO_2) with K_2WO_4, while with [MnCl(**1**)] selective oxidation to HDO is achieved. This selectivity is achieved by exploiting the ability of the microemulsion to compartmentalize the reaction. Thus, by confining the catalyst to the microemulsion droplets (see Figure 2), the loci of the catalyst and the substrate (HD) are matched, while simultaneously those of the catalyst and product (HDO) are mismatched (cf. SANS data). Similar results were obtained in the case of EtSim (Table 1, entries 12 and 13), suggesting that this agent is an 'accurate' simulant for HD.

In general the product distribution and selectivity observed may be explained by considering the *substrate-dependent* changes in mobility observed as a result of oxidation of a sulfide to a sulfoxide, which are defined as ΔD_s^{ox}. The ΔD_s^{ox} values for both highly hydrophilic ($K_{ow} < 0$) *and* lipophilic ($K_{ow} > 3$) substrates are small, as oxidation results in a wholly water-soluble species in the former and in a more polar, but still largely oil-soluble, species in the latter. These diffusion rates help rationalize the above catalysis results. When using lipophilic simulants (e.g., PhSim, NpSim), oxidation affords relatively lipophilic sulfoxides (PhSimO, NpSimO), and since [MnCl(**1**)] resides at the same locus, further oxidation to the sulfone is observed (Table 1, entries 15, 19). More significantly, for lower molecular weight species of intermediate mobility such as HD and EtSim, a large ΔD_s^{ox} value is observed, since sulfoxidation imparts sufficient polarity to convert a lipophile to a hydrophile (see Figure 3b). Thus, the selectivity observed in oxidations of HD and EtSim by [MnCl(**1**)] arises from the oxidation to HDO and EtSimO species that partition into the water phase and are hence less susceptible to further oxidation by the lipophilic droplet-bound catalyst.

Data was also obtained for a wide range of commonly employed simulants and their hydrolysis/oxidation products (Supporting Information). Here it is noted that that while

(51) Meylan, W. M.; Howard, P. H. *J. Pharm. Sci.* **1995**, *84*, 83–92.

hydrolysis of chloroethyl sulfides to $RS(CH_2)_2OH$ species universally results in increased mobility and partition coefficient, the relative change becomes more significant with the lower homologues of the series examined. For example, hydrolysis results in a 6-fold increase in mobility of $C_2H_5SCH_2CH_2OH$ (EtSimOH) compared to EtSim while that of *n*-pentyl derivative (PnSim, $C_5H_{11}SCH_2CH_2Cl$) is only increased by a factor of 1.6. This observation for EtSim is verified by the SANS data described above.

HD and Simulant Oxidation. Surface-Active Catalysts. The interfacial region of a microemulsion is simultaneously exposed to both the aqueous and organic phases. Thus, it was argued that a catalyst localized at the interface should facilitate higher decontamination rates since it is in contact with both substrate and oxidant loci.[52] This concept has been shown to have merit with Richardson *et al.*,[13] demonstrating that interfacially bound bicarbonate, in the form of the counterion to quaternary ammonium surfactants, 'surfoxidants', displayed enhanced rates of catalyzed hydrogen peroxide oxidation rates of aryl alkyl sulfides. It is also understood[35a] that HD reacts with water to form a toxic, complex mixture of sulfonium species, and that hydrolysis products, such as TDG, are involved in the formation of these surface active species. Consequently, there may be a case for oxidizing *all* sulfides in a decontamination protocol, and a surface active catalyst is ideally localized for this role. Accordingly, the more hydrophilic catalyst [MnCl(**3**)] was prepared. Here peripheral morpholine functions impart water solubility and surface activity while a common environment about the metal center is maintained, allowing the rates of sulfide-catalyzed oxidation to be directly compared with those of [MnCl(**1**)] and [MnCl(**2**)]. The activity of [MnCl(**3**)] against HD and simulants is presented in Table 1 (entries 10, 16, 23). It is clear that an increase in catalyst polarity achieves a *higher* rate of sulfide oxidation for *all* substrates, including 1 order of magnitude enhancement for the oxidation of HD to HDO. For HD, in contrast to [MnCl(**1**)], [MnCl(**3**)] now effects rapid oxidation to the sulfone, indicative of an increased exposure of the catalyst to an HDO-enriched aqueous phase. An equimolar ratio of [MnCl(**1**)] and [MnCl(**3**)] (entries, 11, 17, 24) led to an observed rate that was intermediate to that of the single catalyst experiments and the formation sulfone species.

The most striking observation among these results was the essentially identical rates of [MnCl(**3**)]-catalyzed sulfide oxidation, to sulfoxide and sulfone, for HD (entry 10), PhSim (entry 16) and thiodiglycol (TDG, entry 23). This is despite these substrates having substantially differing log K_{ow} (2.41, 3.34, and −0.62, respectively) and D_s values (7.2×10^{-11}, 3.7×10^{-10}, 1.9×10^{-11} m^2 s^{-1}, respectively). The significance of localizing the catalyst at the interface is most dramatically demonstrated by considering that [MnCl(**3**)] also oxidized substrates such as NpSim and the sulfoxide of TDG (TDGO, $\log_{10} K_{ow} = -2.76$). Thus, substrates of K_{ow} values differing by a factor of 10^7 (and a D_s range of 10^2) are effectively oxidized by [MnCl(**3**)] within a microemulsion system. These results also lend credence to the notion that the compartmentalization of the reaction has been used to good effect in the case [MnCl(**1**)], since by shifting the catalysts from the core to the interface, as in the case of [MnCl(**3**)], low molecular weight sulfoxides (e.g., HDO and EtSimO) suffer from overexposure to the activated catalyst, as verified by loss of sulfoxide selectivity observed in [MnCl(**3**)]-catalyzed reactions.

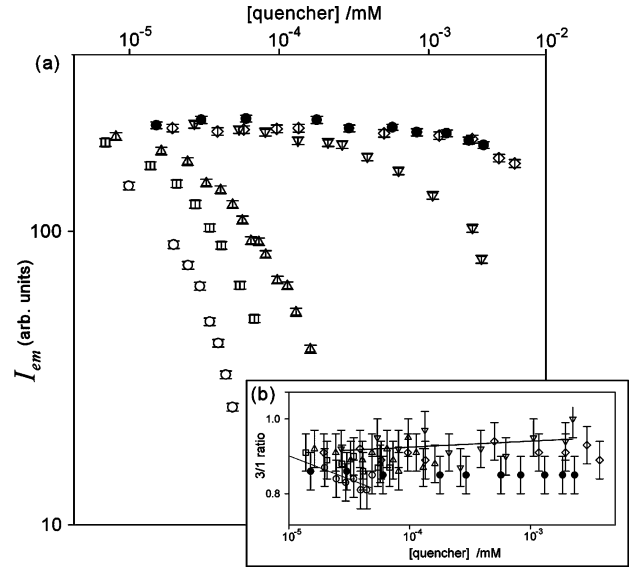

Figure 4. (a) The intensity of SDS5T solubilized pyrene emission at 396 nm as a function of quencher concentration: [MnCl(**1**)] (○), [MnCl(**3**)] (□), $[Cu(L)]Cl_2$ (aq) (△, L = 1-(2-hydroxytetradecyl)-1,4,7,10-tetraazacyclononane[55]), $Cu(NO_3)_2$ (aq) (▽), $Mn(NO_3)_2$ (aq) (◇), and K_2WO_4(aq) (●). (b) The inset shows the ratio of the third to first vibronic peak of the pyrene probe of the same data.

Measurement of Catalyst Location. The PGSE-NMR data give an accurate representation of the partitioning of the catalyst and simulant between the aqueous and micellar structure. It, however, cannot inform on the location within the micellar structures viz. interface bound or buried "deep" within the hydrophobic core. The SANS/SAXS study unfortunately was unable to *definitively* resolve this issue, although the presence of peaks in the various data sets gives an unequivocal indicator of solubilized hydrophobic materials, since a careful analysis of the absolute intensities could not reproduce that expected from assuming the simulants or catalysts were entirely located on any one phase but to varying degrees reflecting their relative hydrophobicities. Taken together, the PGSE-NMR and SANS/SAXS comparison is convincing, and the loci of the various catalysts may be inferred from the catalysis results. A more satisfying analysis arises from the relative efficiency of the various metals to quench the fluorescence of pyrene, indicative of the colocalization of the interfacially accessible pyrene and the catalyst.

Pyrene is a hydrophobic molecule that has been widely used to study the micellization of surfactants. Two characteristics of the fluorescence were employed here: the ratio of the third to first vibronic peak which gives a direct measure of the polarity of the location of the probe, and the intensity of the fluorescence as a function of the concentration of an added quencher molecule.[53] Figure 4a displays the intensity of the pyrene fluorescence as a function of metal ion concentration, the quencher, while Figure 4b reports the 3/1 ratio of the pyrene in the same systems. Considering Figure 4b first, the magnitude of the 3/1 ratio and their invariance with the quencher concentration clearly demonstrates that the pyrene resides in a

(52) For a recent example of a surface active Mn(III) salen species, see Kureshy, R. I.; Khan, N. H.; Abdi, S. H. R.; Patel, S. T.; Iyer, P. K.; Jasra, R. V. *Tetrahedron Lett.* **2002**, *43*, 2665–2668.

(53) (a) Humphry-Baker, R.; Gratzel, M.; Moroi, Y. *Langmuir* **2006**, *22*, 11205–11207. (b) Grieser, F.; Tausch-Treml, R. *J. Am. Chem. Soc.* **1980**, *102*, 7258–7264. (c) Graetzel, M.; Thomas, J. K. *J. Am. Chem. Soc.* **1973**, *95*, 6885–6889.

hydrophobic environment and that inclusion of the catalyst has only a negligible effect, if any, on the structure of the micellar aggregate. In Figure 4a it is also clear that K_2WO_4 (aq), $Mn(NO_3)_2$ (aq), and $CuCl_2$ (aq) have little effect on the fluorescence intensity; the observed decrease exhibited by the K_2WO_4 (aq) and $Mn(NO_3)_2$ (aq) may be accounted for entirely due to the dilution of the sample by the aliquots of the quencher solution. The decrease in intensity caused by the addition of $CuCl_2$ (aq) is greater than that expected by dilution, and therefore some quenching of the fluorescence by the copper occurs. This observation indicates that (a) the pyrene is accessible to the aqueous phase and (b) that hydrated Cu^{2+} ions are present to some degree at the micelle surface. This is not unexpected for an anionic surfactant. This observation partially explains the high activity of [MnCl(**1**)] observed in the oxidation of TDG (Table 1, entry 22). The copper-based metallosurfactant is rather different to the simple copper salt, with the efficiency of the fluorescence quenching significantly increased, undoubtedly due to the (controlled) concentration of the metal ions at the micelle surface on account of the hydrophobic moiety.[54] Indeed, all the droplet-constrained metal complexes are efficient quenchers of fluorescence. MnCl(**1**) is the most lipophilic quencher and is correspondingly the most efficient.

If one defines the efficiency of quenching as the gradient of the data in Figure 4a (plotted in a linear fashion, not the double logarithmic representation as presented), the [MnCl(**1**)] is some 50% more efficient than its closely related analogue [MnCl(**3**)], indicating a more pronounced overlapping of the locations of pyrene and the former quencher. Thus, [MnCl(**1**)] spends more time in a location occupied by the pyrene, principally the hydrophobic core, although the copper metal fluorescence results do demonstrate that it is accessible to the solution phase. Further, [MnCl(**1**)] and [MnCl(**3**)] are several orders of magnitude better at quenching the pyrene fluorescence than the free $Mn(NO_3)_2 \cdot 6H_2O$, and it is therefore reasonable to assume that [MnCl(**3**)] is more surface active, i.e., is present at the interface of the swollen micelle.

Conclusions

In this work it has been demonstrated that rapid oxidation of HD and simulants can be achieved at low, safe, and noncorrosive H_2O_2 concentrations. The observation that K_2WO_4 (aq)-catalyzed oxidations of HD occur at appreciable rates is seemingly in contradiction with the lipophilic nature of HD. Further, the high mobility of HD implies greater aqueous exposure and explains the activity of K_2WO_4 and other previously described water-soluble catalysts. The efficacy of [MnCl(**1**)] suggests an interfacial oxo transfer process from peroxide to catalyst. In the current system selectivity may be achieved at the expense of rate using a more hindered ligand such as [MnCl(**2**)] or, in the case of HD or EtSim oxidations, by using the lipophilic [MnCl(**1**)] and allowing the enhanced water partitioning of the HDO product to protect it from further oxidation. The surface-active catalyst [MnCl(**3**)] achieves enhanced rates of oxidation of all sulfides, irrespective of polarity, albeit at the expense of selectivity. The control over selectivity that may be achieved in this system is best illustrated in the differing activity of

Scheme 2. Summary of the Activity of (a) Water-Soluble (K_2WO_4), (b) Oil-Soluble ([MnCl(**1**, **2**)]), and (c) Surface-Active ([MnCl(**3**)]) Catalysts in Microemulsion Media[a]

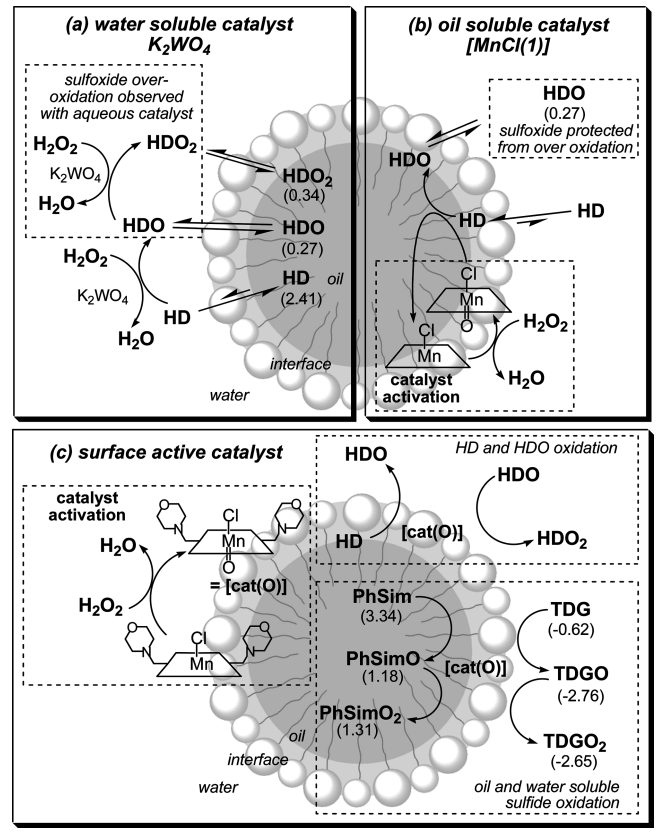

[a] Values in parentheses are calculated oil−water partition coefficients (log K_{ow} values).

[MnCl(**1**)] compared to that of [MnCl(**3**)]. Here it is apparent that use of an ethane backbone in the ligand framework renders both catalysts capable of sulfide oxidation to the sulfone, but that for low molecular weight species (HD, EtSim) the enhanced water partitioning results in selective sulfoxide formation for the nonsurface active [MnCl(**1**)].

Collation of these observations suggests a number of equilibria that govern the partitioning of HD and its oxidation products in microemulsion systems (Scheme 2). The observations that K_2WO_4 promotes over oxidation to sulfone while [MnCl(**1**)] achieves the selective oxidation of HD to HDO may both be explained by noting the lower K_{ow} and more significant D_s values of HDO relative to HD. The lack of sulfone formation with [MnCl(**1**)] implies that HDO is too polar to penetrate the oil core of the microemulsion droplets. Rapid sulfoxide and sulfone formation with [MnCl(**3**)] indicates that oxidation with this catalyst occurs within the interfacial region, which is indirectly confirmed by the universality in the oxidation behavior of HD, PhSim, and TDG (see Table 1). In essence, by 'matching' the locus of the catalyst and the sulfide substrate, and 'mismatching' that of the sulfoxide product, enhanced rates of reaction and selective oxidation can be achieved. Previous workers have largely used microemulsions as a means of dispersing agent. Here it has been shown that the use of a microemulsion not only can have a significant effect on rate, via dispersion, but also on product speciation via partioning control. Moreover, hydrophobic sulfides such as PhSim and NpSim are effectively oxidized, although at the expense of selectivity, by oil soluble and surface active catalysts. These

(54) For an account of metallosurfactant quenching phenomena in micellar systems, see Humphry-Baker, R.; Moroi, Y.; Grätzel, M.; Pelizzetti, E.; Tundol, P. *J. Am. Chem. Soc.* **1980**, *102*, 3689–3692.

(55) Griffiths, P. C.; Fallis, I. A.; Willock, D. J.; Paul, A.; Barrie, C. L.; Griffiths, P. M.; Williams, G. M.; King, S. M.; Heenan, R. K.; Gorgl, R. *Chem. Eur. J.* **2004**, *10*, 2022–2028.

are important observations when considering the decontamination of the comparably lipophilic sesquimustards ($ClCH_2CH_2S$-$(CH_2)_nSCH_2CH_2Cl$; log $K_{ow} = 2.99-4.46$ for $n = 2-5$), which may be present as a byproduct of the manufacturing (Levinstein) process. The work highlights the importance of interfacial reactivity of a surface-active catalyst such as [MnCl(**3**)]; by programming the locus of the catalyst within the microemulsion to simultaneously expose catalyst, agent, hydrolysis, and oxidation products to a source of oxidant, a significantly enhanced rate of decontamination is achievable. We will explore the mechanistic and kinetic implications of these observations in a subsequent paper.

Acknowledgment. We thank Harry McEvoy and Kenneth Kinear (DSTL) for valuable discussion. STFC are acknowledged for the provision of neutron beamtime, EPSRC for funding (GR/S98771/01, EP/C53090X/1, EP/G006156/1, EP/C013220/1, GR/S25456/01), and the Cardiff Institute for Tissue Engineering and Repair (CITER) for the provision of mass spectrometry facilities.

Supporting Information Available: Preparation of catalysts and simulants, PGSE data, complete listing of D_s and K_{ow} values for all simulants and agents, MS analyses of EtSim and HD in microemulsion, and detailed SANS/SAXS analysis. This material is available free of charge via the Internet at http://pubs.acs.org.

JA901872Y